Microstructure and adhesion of 100Cr6 steel coatings thermally sprayed on a 35CrMo4 steel substrate

Article *in* Surface and Coatings Technology · June 2008

DOI: 10.1016/j.surfcoat.2008.04.039

5 authors, including:

Bradai Mohand Amokrane
Université de Béjaïa
43 PUBLICATIONS **54** CITATIONS
SEE PROFILE

Muriel Braccini
French National Centre for Scientific Research
68 PUBLICATIONS **433** CITATIONS
SEE PROFILE

Abdelaziz Ati
Université de Béjaïa
24 PUBLICATIONS **149** CITATIONS
SEE PROFILE

Bounar Nedjemeddine
University of Jijel
14 PUBLICATIONS **42** CITATIONS
SEE PROFILE

Available online at www.sciencedirect.com
ScienceDirect
Surface & Coatings Technology 202 (2008) 4538–4543
SURFACE & COATINGS TECHNOLOGY
www.elsevier.com/locate/surfcoat

Microstructure and adhesion of 100Cr6 steel coatings thermally sprayed on a 35CrMo4 steel substrate

Mohand Amokrane Bradai [a], Muriel Braccini [b], Abdelaziz Ati [a,*], Nedjemeddine Bounar [c], Abderrahim Benabbas [c]

[a] Laboratory of Technology of Materials and Engineering of the Processes, Faculty of Science and Science Engineering. University of Béjaia, 06000, Algeria
[b] SIMAP/INPG, CNRS/UJF-1130, Rue de la Piscine BP 75, 38402 Saint-Martin d'Hères, France
[c] Laboratory of Interaction Materials and Environment, University of Jijel, 18000, Algeria

Available online 10 April 2008

Abstract

Thermally sprayed of 100Cr6 steel coatings are widely used to combat degradation of components and structures due to mechanical wear. In this paper, the microstructure and adhesion energy of 100Cr6 steel coatings thermally sprayed on a 35CrMo4 steel substrate are investigated. The microstructure characteristics of the deposits are studied using the combined techniques of X-ray diffraction (XRD), optical microscopy, scanning electron microscopy (SEM) including energy-dispersive spectroscopy (EDS). The practical work of adhesion of flame-sprayed 100Cr6 on steel substrate is determined using a four-point *delamination* bending test. The influence of a molybdenum bond coat on the adhesion is also studied. Microstructure suggests that the coating is mainly constructed by splats of γ-phase (fcc) and FeO. Phase analysis also confirms that during spraying process, a stable α-phase (bcc) was transformed into a new γ-phase (fcc). The highest values of the fracture energy are obtained for the 35CrMo4 substrate/100Cr6 steel deposit type samples. On the contrary, when a molybdenum bond coat is introduced (composite system 35CrMo4 substrate/Mo bond coat/100Cr6 steel deposit), the fracture energy decreases in a ratio of approximately three. So, the presence of a Mo bond coat as a barrier between the coating and the substrate has a negative role on the adhesion.

Keywords: Thermal spraying; Microstructure; Phase; Bond coat; Coatings; Adhesion

1. Introduction

Thermal spray coating represents an important and cost-effective technique for tailoring the surface properties of engineering components with a view to enhance their durability and performance under a variety of operating conditions [1,2]. It is also used to repair and refurbish worn or otherwise degraded parts, to restore a part to its original dimensions and improve its surface properties. Adhesion is one of the most important characteristics used to determine the quality of the coating [3–6]. Coating quality was characterized using a number of different tests [7,8]: one of them is the four-point "delamination" bending test [9]. In the present work, the role of the molybdenum bond coat on the practical work of adhesion of the100Cr6 steel deposit is investigated. In this goal, two types of composite system, A and B, have been prepared: (A) (35CrMo4 substrate/Mo bond coat/100Cr6 coating) and (B) (34CrMo4 substrate/100Cr6 coating). First, the aim of this work is to explore the results of the microstructure and morphology of coating using a flame spray technique. Produced coatings are characterized by X-ray diffraction (XRD) analysis and scanning electron microscopy (SEM) with energy-dispersive X-ray spectrometry (EDS). Second, the adhesion of flame-sprayed 100Cr6 on 35CrMo4 steel substrate is determined using a four-point bending test. The influence of a molybdenum bond coat on the adhesion is considered.

2. Experimental procedures

2.1. Material and spray conditions

The common substrate used is a 35CrMo4 steel with the dimensions of $60\times10\times4$ mm^3. Two types of sample are realized: (A) 35CrMo4 steel substrate/Mo bond coat/100Cr6 steel coating. To point out the specific effect of the molybdenum

* Corresponding author. Tel./fax: +213 34 21 51 05.
E-mail address: aziati_3000@yahoo.fr (A. Ati).

0257-8972/$ - see front matter © 2008 Elsevier B.V. All rights reserved.
doi:10.1016/j.surfcoat.2008.04.039

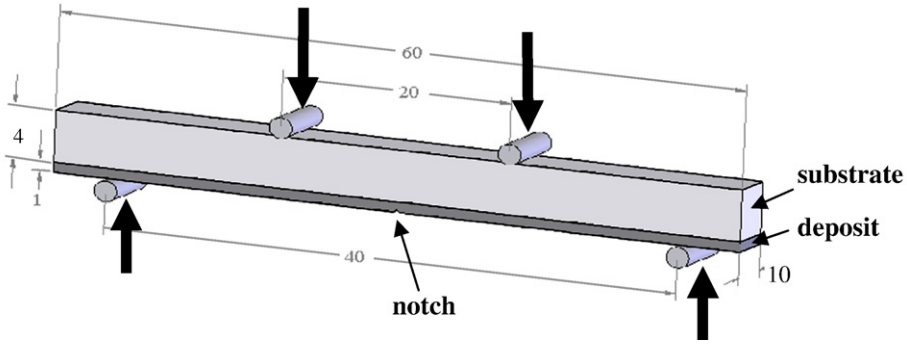

Fig. 1. Adhesion testing; experimental set-up for the four-point *delamination* bending test.

bond coat, the second sample is covered by a 100Cr6 steel deposit directly on the substrate, (B) 34CrMo4 substrate/100Cr6 coating. Prior to deposition, the samples are cleaned, degreased and grit blasted according to usual procedures [10]. The metal deposits are performed by means of a gun with a standard flame-wire "Mark 60" with a thickness of 1 mm. For the molybdenum deposit, the bond coat is 0.1 mm thick.

For the projection of molybdenum, an oxyacetylene flame is used. The fuel is acetylene under a pressure of 1.2 bars and the combustive gas is oxygen used under a pressure of 4 bars. An oxypropane flame is prepared for the projection of 100Cr6 steel by using a pressure of 3 bars for the propane gas. The projection pressure of the molten metal is 4.5 bars for steel and 3.8 bars for molybdenum. The projection parameters used to form the composite systems A and B are the following: projection distance 140 mm, wire speed 0.015 m/s. These projection parameters are those indicated in the technical chart of the SNC ATRA Company [11].

2.2. Characterization techniques

2.2.1. Coating characterization. As-received coatings are cross-sectioned, ground using SiC papers with grit sizes down to 2400 and finally polished with 1 μm alumina. Microstructure of the coatings is observed using optical microscopy and scanning electron microscopy (PHILIPS XL 30 SEM). Chemical composition is analyzed using an energy-dispersive spectroscopy (EDX–SEM) and phase analysis using an X-ray diffraction (XRD). The XRD spectra brought back in this work are recorded by using a chromium anticathode, starting from a polished side cut of the sample. The X-ray beam passing through a collimator of 0.8 mm in diameter can be applied to the desired zone, which makes it possible to separate the contribution of the substrate from that of the deposit. Identification of the crystalline phases is made by comparison of the observed lines with those of the suitable phases contained in the data base PDF2.

2.2.2. Adhesion testing. From the microscopic point of view, adhesion is due to reversible interactions (Van Der Waals, covalent, ionic) which can be established at the coating–substrate interface [12,13] and corresponds to the work of adhesion, a thermodynamic parameter. From the mechanical point of view, the practical work of adhesion corresponds to interfacial fracture energy. It is of a macroscopic nature and includes all energies (mechanical, electrical, thermal) that are dissipated in the different materials (layer, bond coat, substrate) during the delamination. In this study, the fracture energy of the deposited material on the substrate is measured using a four-point 'delamination' bending test [14–16] in agreement with the European standards.

This test consists of a notch flexural beam. The specimen is a bi (or more) material beam with a central notch (Fig. 1). In our case, the coating is stiff enough so that we do not have to glue a stiffener to enhance the delamination: this allows to suppress energy dissipation in an adhesive. Moreover, due to the brittle behaviour of the coating, only a short notch is necessary to initiate fracture. The sample is placed in a bending set-up where the distances between inner load lines is 20 mm and between outer load lines is 40 mm (Fig. 1). Tests are conducted with a constant displacement rate of 0.5 mm min^{-1}. Hence, a CCD camera allows to record beam cross-section all along its deformation.

During the load, a crack initiates at the notch, first in the coating and then propagates symmetrically in the coating–substrate interface. This crack is subject to constant moment conditions and propagates in steady state conditions. The strain energy release rate G_{IF} can be evaluated analytically using Euler–Bernoulli beam theory as following (Eq. (1)) [8,16]:

$$G_{IF} = \frac{p_c^2 l^2 (1-\nu_s^2)}{E_s e^3 b^2} \times \frac{3}{2}\left\{\frac{1}{(e_s/e)^3} - \frac{\lambda}{(e_d/e)^3 + \lambda(e_s/e)^3 + 3\lambda(e_d e_s/e^2)(e_d/e + \lambda(e_s/e))^{-1}}\right\} \quad (1)$$

where

$$\lambda = \frac{E_s(1-\nu_d^2)}{E_d(1-\nu_s^2)} \quad (2)$$

and p_c is delamination strength (Newton); E_s is substrate Young's modulus (210 GPa for 35CrMo4 steel); E_d is deposit Young's modulus (210 GPa for 100Cr6 steel); ν_s is substrate Poisson's ratio (0.3 for 35CrMo4 steel); ν_d is deposit Poisson's ratio (0.3 for 100Cr6 steel); e_s is substrate thickness = 4 mm e_d is deposit thickness = 1 mm; $e = e_s + e_d = 5$ mm; b is sample widths = 10 mm; and l is distance between internal and external alumina blocks = 10 mm. The fracture (or delamination) strength p_c is determined from the load–displacement curve obtained during the test. It generally corresponds to a plateau, but in some case only an inflexion on the curve is observed.

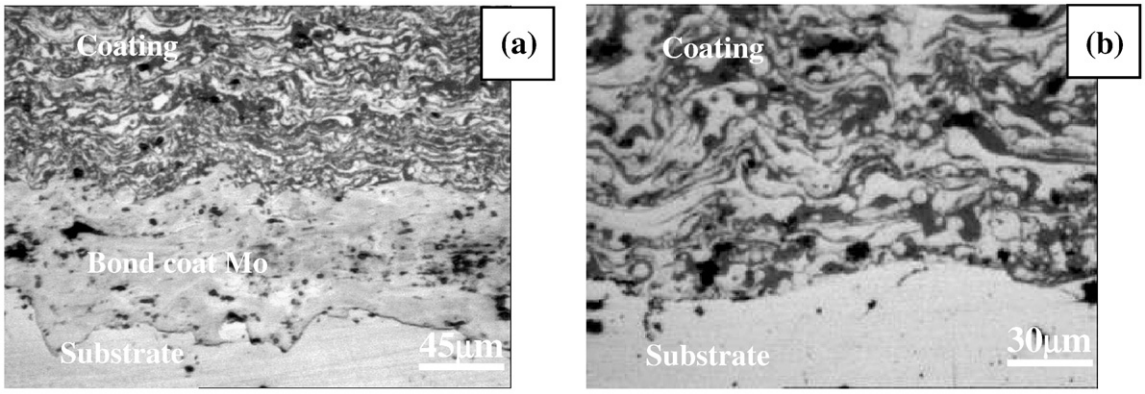

Fig. 2. Morphology of a) the 100Cr6 steel coating and the Mo bond coat, b) the 100Cr6 steel coating realized without bond coat. Deposit has a lamellar structure.

This is our case: this inflexion corresponds to the deviation of the crack in the coating–substrate interface as verified thanks to the CCD record. The determination of the Young's modulus E of the used materials (35CrMo4 substrate, 100Cr6 coating, Mo bond coat), needed for this analytical calculation, has been done in a series of experimental studies using a test based on the magnetic resonance of a vibrating blade [8,12,17]. The blade is obviously constituted of the specific material to study. This method uses the relations which exist between the vibratory behaviour of a material and its elastic properties. It consists on measuring the resonance frequency of a material having a blade shape and submitted to vibration [16].

3. Results and discussion

3.1. Microstructure investigation

3.1.1. Optical microscope observations

Polished cross-sections of the coatings are examined in an optical microscope. The micrographics presented on Fig. 2 illustrate the morphology of the deposit of hypereutectoid steel of nuance 100Cr6 and that of bond coat in molybdenum. The deposits obtained have a lamellar morphology. Indeed, the molten particles are crushed and spread out over the substrate or particles already deposited and form fine plates which adapt to the irregularities of the surface. The observations of the interface between the substrate and the molybdenum bond coat (Fig. 2a) reveal a good adhesion of the sublayer with the deposit although their respective coefficients of thermal expansion α are very different. Their ratio is approximately 2 since $\alpha = 10.8 \times 10^{-6}\ K^{-1}$ for the hypereutectoid steel deposit and $5.2 \times 10^{-6}\ K^{-1}$ for this bond coat [18]. In addition, the utility of the Mo under layer coating, applied to the restoration of worn surfaces of crank pins and crankshaft bearings, can really be questioned since the linear dilatation coefficient of molybdenum ($5.2 \times 10^{-6}\ K^{-1}$) is far from those of the final 100Cr6 steel coating ($10.8 \times 10^{-6}\ K^{-1}$) and of the 35CrMo4 steel substrate ($12 \times 10^{-6}\ K^{-1}$). This consideration led the present authors to test the quality of the adhesion of the composite system B fabricated without Mo bond coat (Fig. 2b). The observation of micrographs exhibiting transverse sections reveals a perfect interface between the coating and the substrate.

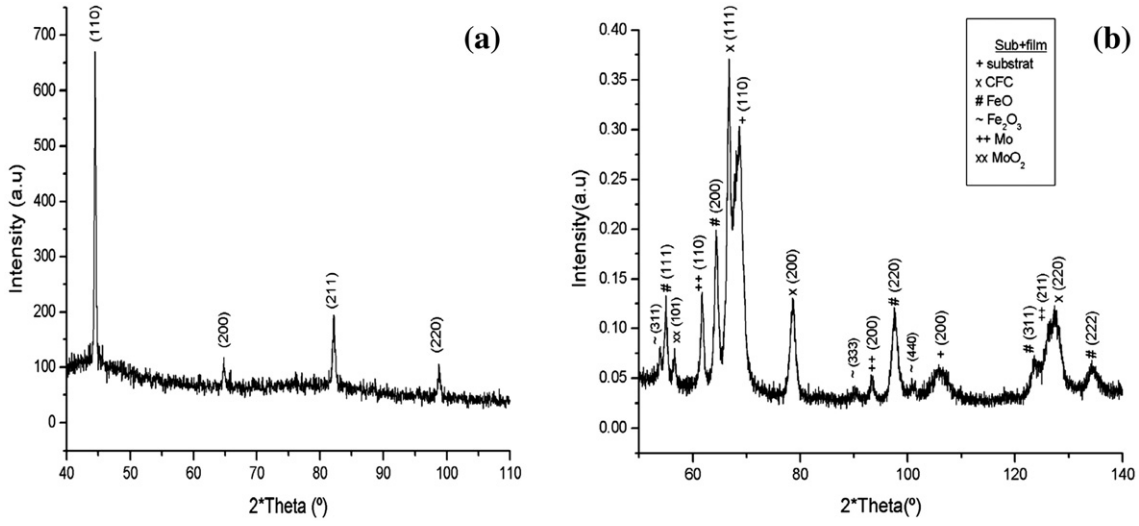

Fig. 3. XRD diagrams of (a) 100Cr6 wire, (b) composite system (35CrMo4 steel substrate/Mo bond coat/100Cr6 steel coating). (The JCPDS cards for the phases detected in XRD patterns are (bcc) phase α: 06-0696, (fcc) phase γ Fe(C) austenite: 31-0619, FeO: 03-0968, γ-Fe_2O_3: 02-1047, Mo: 42-1120, MoO_2: 01-0615).

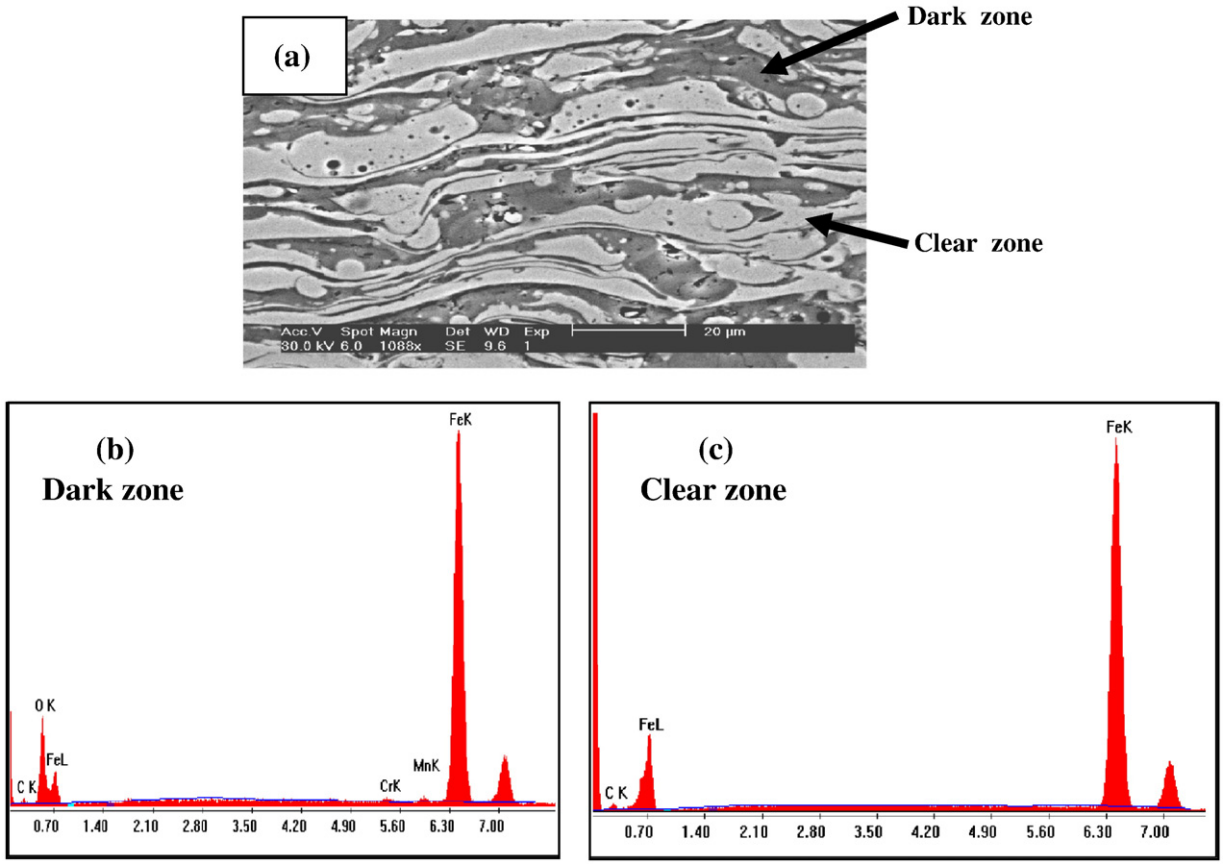

Fig. 4. EDS analysis of the 100Cr6 steel coating (a) SEM image, (b) and (c) EDS analysis on dark zone and clear zone respectively.

3.1.2. X-ray diffraction analysis (XRD)

The microstructure of the 100Cr6 steel flame-sprayed in air and mixed with the Mo bond coat is investigated by X-ray diffraction. The identification of the crystalline phases is made by comparison between the lines observed and those of the suitable phases contained in the data base PDF2. The Fig. 3a shows the diffractogram obtained exclusively from the wire 100Cr6 steel. The observed peaks are characteristic of a body-centred cubic (bcc) structure; this result was expected owing to the composition of the used 100Cr6 steel. The refinement of the lattice parameter, by taking into account the shift of the spectra related to the position of the sample, leads to the value of $a=2.872(5)$ Å. For the composite system A: (35CrMo4 substrate/Mo bond coat/100Cr6 steel coating), the application of the X-ray beamed on the common area of the substrate, Mo bond coat and the deposit, gives rise to the diffractogram of the Fig. 3b. We easily recognize on the one hand the lines (110) and (200) of the substrate and on the other hand the characteristic lines of the molybdenum and its MoO_2 oxide in the bond coat. The lines of molybdenum are used to correct the shift of this diffractogram which allows the identification of the remaining lines. Indeed, we note the presence of face-centred cubic (fcc) austenitic steel and of iron oxide FeO, with the lattice parameters $a=3.613(7)$ Å and $a=4.302(5)$ Å respectively. We note also the presence, in small proportion, of the metastable form γ-Fe_2O_3. According to these results, one can make the following comments: The adoption of the fcc structure, more compact than the bcc one, in the deposit is independent of the structure of the starting used steel. But, it is related to the spraying process which can be assimilated to a short pressure followed by a hardening. This is particularly true for the samples (A) and (B) where the employed steel wire is of bcc

Table 1
EDX ZAF quantification

(b) Dark zone							(c) Clear zone						
Element	wt.%	at.%	K-ratio	Z	A	F	Element	wt.%	at.%	K-ratio	Z	A	F
C	7.32	18.69	0.0164	1.1084	0.2020	1.0006	C	11.49	37.65	0.0240	1.1380	0.1834	1.0006
O	22.22	42.59	0.0829	1.0926	0.3404	1.0028	Fe	88.51	62.35	0.8716	0.9780	1.0070	1.0000
Cr	0.35	0.20	0.0043	0.9468	0.9994	1.3226							
Mn	0.55	0.31	0.052	0.9315	1.0088	1.0000							
Fe	69.57	38.21	0.6704	0.9509	1.0134	1.0000							

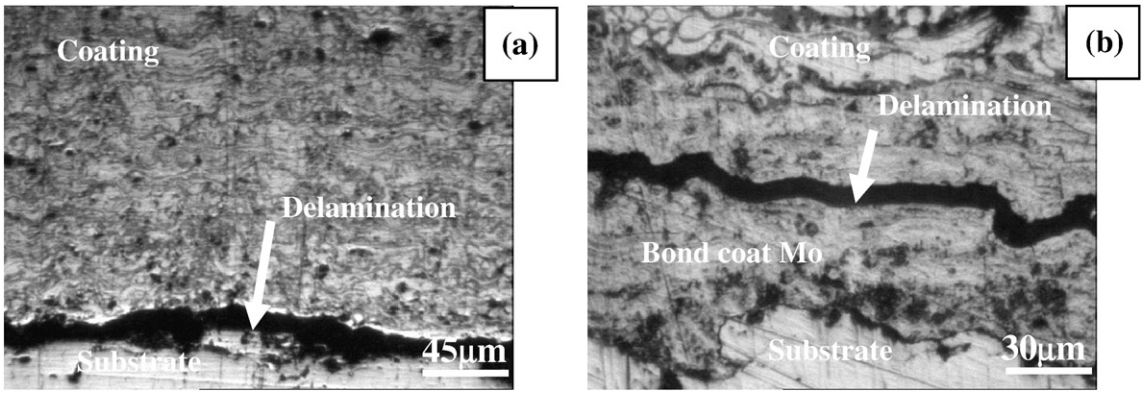

Fig. 5. Delamination crack of (a): (34CrMo4 substrate/100Cr6 coating) and (b): (35CrMo4 substrate/Mo bond coat/100Cr6 coating).

structure. Furthermore, the formation of iron oxide FeO in sample (A) and (B) is due to the trapping of oxygen by the steel deposited on the substrate; this oxygen then reacts with iron during cooling which leaves porosity in the texture. Indeed, micrographics show a correlation between the density of pores and the amount of the dark phase which is associated to iron oxide FeO. The clear phase in the micrographics is thought to be the fcc steel mentioned above. During spraying process, the stable α-phase (bcc) is transformed to the new γ-phase (fcc). It has been suggested that the γ-phase (fcc) always homogeneously nucleates in the rapid quenching of completely melted droplets because its critical free energy for nucleation from the liquid is less than that of the α-phase.

3.1.3. Edx–sem

Chemical composition analysis of the coating achieved by EDX–SEM technique confirms the DRX results (Fig. 4). Local EDX spectrum from the clear zone (Fig. 4c) exhibits only iron and carbon elements corresponding to the γ-phase (fcc) while that of the dark zone shows also the presence of oxygen with atomic ratio corresponding to the FeO phase (Table 1b).

The EDX ZAF of two compounds forming the coating during spraying process is presented in Table 1.

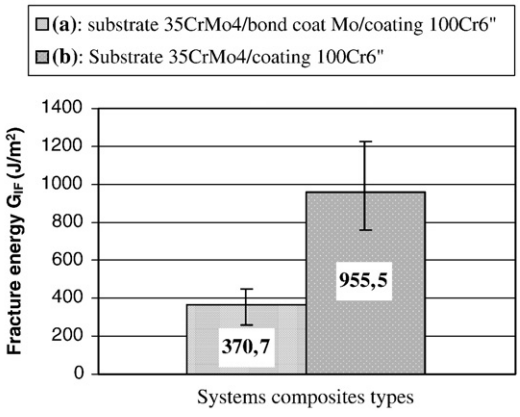

Fig. 6. Fracture energy variation according to samples of (A) 35CrMo4 substrate/Mo bond coat/100Cr6 steel coating and (B) 35CrMo4 steel substrate/100Cr6 steel coating. Longitudinal bars show maximum and minimum of the measured fracture energy.

3.2. Coatings adhesion

In order to study the effect of a Mo bond coat on the adhesion of the 100Cr6 coating on a 35CrMo4 substrate, specimen with and without bond coat have been elaborated. To be sure of reproducibility, four samples of each material are tested. For samples without bond coat (35CrMo4 substrate/100Cr6 steel coating), crack initiates at the notch and then deviates and propagates along the coating–substrate interface all during the test. In spite of its separation from steel substrate, generally the coating is still compact as shown in Fig. 5a. In the case of samples with Mo bond coat (35CrMo4 substrate/Mo bond coat/100Cr6 steel coating), no effective fracture occurs at the interface of the different samples but cracks and micro cracks appear in the molybdenum coating. These cracks run in the middle of the bond coat but no separation of the coating was observed (Fig. 5b) [19]. The highest values of the fracture energy are obtained for the: 35CrMo4substrate/100Cr6 steel coating: the fracture energy is 955 ± 200 J/m^2 (Fig. 6).

For samples with of a Mo bond coat, the fracture energy is about 371 ± 100 J/m^2 (Fig. 6). This lower adhesion can be linked to the formation of pores and MoO_2 type oxides in the bond coat, that are brittle intermediate phases (confirming by X-ray diffraction). In addition, the good adhesion in the samples without bond coat can be explained owing to the fact that the substrate and the deposit are of comparable compositions (low alloy steel with chromium and molybdenum) and consequently have a good miscibility during fusion. They have also similar elastic properties and thermal expansion coefficients [20,21].

4. Conclusion

In this study, microstructure and phase composition in the 100Cr6 coating are investigated. Dense coating was received; however, defects such as cracks and incompletely melted particles should be minimized by adjusting spraying parameters. Phase analysis using X-ray diffraction confirms that during spraying process, a stable α-phase (bcc) is transformed to a new γ-phase (fcc). It has been suggested that the γ-phase (fcc) always homogeneously nucleated in the rapid quenching of completely melted droplets because of its critical free energy for nucleation from the liquid was less than that of the α-phase.

The work of adhesion of flame-sprayed 100Cr6 on steel substrate is determined using a four-point "delamination" bending test. The highest values of the fracture energy are obtained for the samples without Mo bond coat (35CrMo4 substrate/100Cr6 deposit): an average value of 955 ± 200 J/m^2 is obtained. For samples with a Mo bond coat, the fracture energy decreases to 370 ± 100 J/m^2. This lower adhesion can be linked to the formation of pores and MoO_2 type oxides in the bond coat. So, the introduction of a Mo bond coat as a barrier between the coating and the substrate has not improved the adhesion. In addition, the good adhesion of the substrate–coating interface in the samples without bond coat can be explained owing to the fact that the substrate and the deposit are of comparable compositions (low alloy steel with chromium and molybdenum) and consequently have a good miscibility during fusion. Moreover, the dilatation coefficients of the two materials are of the same order of magnitude, namely 10.8×10^{-6} K^{-1} for 100Cr6 deposit and 12×10^{-6} K^{-1} for 35CrMo4 substrate.

References

[1] L. Pawlowski, The Science and Engineering of Thermal Spray Coatings, John Wiley, Chichester, England, 1995.
[2] P. Fauchais, A. Vardelle, B. Dussoubs, J. Therm. Spray Technol. 10 (2001) 44.
[3] A. Hjorhhede, A. Nylund, Surf. Coat. Technol. 184 (2004) 208.
[4] C. Godoy, E.A. Souza, M.M. Lima, J.C.A. Batista, Thin Solid Films 420–421 (2002) 438.
[5] A. Rabiei, D.R. Mumm, J.W. Hutchinson, R. Schweinfest, M. Ruhle, A.G. Evans, Mater. Sci. Eng., A Struct. Mater.: Prop. Microstruct. Process. 269 (1999) 152.
[6] S. Sampath, X.Y. Jiang, J. Matejicek, A.C. Leger, A. Vardelle, Mater. Sci. Eng., A Struct. Mater.: Prop. Microstruct. Process. 272 (1999) 181.
[7] G. Marot, J. Lesage, Ph. Démarécaux, M. Haddad, St. Siegmann, M.H. Staia, Surf. Coat. Technol. 201 (2006) 2080.
[8] M. Laribi, N. Mesrati, A.B. Vannes, D. Treheux, Surf. Coat. Technol. 166 (2003) 206.
[9] M. Laribi, A.B. Vannes, D. Treheux, Surf. Coat. Technol. 200 (2006) 2704.
[10] Molybdenum coating characteristics, Technical Bulletin of Metalisation Spray Co. Issue: 7/03–96.
[11] 100Cr6 coating characteristics and parameters spray conditions, Technical Bulletin of Company S.N.C ATRA (Algeria).
[12] V. Guipont, Experimental determinations of residual stresses in materials realized by brazing, PhD thesis. No 94-50, (1994), E.C. Lyon, France (in French).
[13] M. Dupeux, Méc. Ind. 5 (2004) 441.
[14] J. Lesage, D. Chicot, D. Judas, M. Zampronio, et al., Matér. Tech. 9–10 (1999) 29 in French.
[15] M. Laracine, C. Bignon, M. Lormand, J. Hernandez, et al., J. Phys. 12 (1987) 147.
[16] P.G. Charalambides, J. Lund, A.G. Evans, R.M. McMeeking, J. Appl. Mech. 56 (1989) 77.
[17] G. Lallemand-Tallaron, Study of the microstructure and adhesion of spinelles coatings formed by plasma spraying, PhD thesis. No 96- 58, (1996), EC Lyon. France.
[18] J. Hochman, Tech. l'Ing. M328 (1) (1986) 1.
[19] M.A. Bradai, A. Ati, Alger. J. Adv. Mater. 3 (2006) 115.
[20] M. Dupeux, La Revue de Métallurgie—CIT/Sciences et Génie des Matériaux, no. 2, 2004, p. 83.
[21] M.C. Sahour, M. Laracine, A.B. Vannes, La Revue de Métallurgie—CIT/Science et Génie des Matériaux, 2004, p. 715.